The disordered magnetic structure in the triangular-lattice XY-antiferromagnet $CsMnBr_3$ derived from the zero-field spectrum of Br nuclear magnetic resonance

1996 J. Phys.: Condens. Matter 8 4063

(http://iopscience.iop.org/0953-8984/8/22/010)

J. Phys.: Condens. Matter **8** (1996) 4063–4070. Printed in the UK

The disordered magnetic structure in the triangular-lattice *XY*-antiferromagnet $CsMnBr_3$ derived from the zero-field spectrum of Br nuclear magnetic resonance

Xun Xu†, Kunihide Okada†, Muneaki Fujii†, Takeji Kubo‡ and Yoshitami Ajiro§

† Department of Physics, Kumamoto University, Kurokami 2-39-1, Kumamoto 860, Japan
‡ Department of Physics, Nara Education University, Takabatake, Nara 613, Japan
§ Department of Applied Physics, Fukui University, Bunkyo 3-9-1, Fukui 910, Japan

Received 20 October 1995, in final form 9 April 1996

Abstract. The Br NMR in the triangular-lattice antiferromagnetic $CsMnBr_3$ is investigated in the ordered state at low temperatures. Two distinct peaks of the Br NMR spin-echo spectrum were observed at 36.0±0.5 MHz and 43.0±0.5 MHz accompanied by a broad signal ranging from 34 to 55 MHz in zero field. The peak frequencies are independent of temperature and the ratio of the frequencies is the same as that of the quadrupole moments of ^{81}Br and ^{79}Br. This suggests that the quadrupole resonance of Br is perturbed by the distribution of the internal magnetic field. Theoretical results obtained under the assumption that the Mn spins have disordered structure in the *c*-plane due to the frustration effect agree with the experimental data.

1. Introduction

The antiferromagnetic planar (*XY*-) model of a triangular lattice is one of the two-dimensional (2D) frustrated spin systems that exhibit many types of phase structure. From the theoretical point of view, the magnetic phase transition is closely related to the symmetry breaking of the helicity or chirality (Z_2) in addition to the *XY*-symmetry (S_1), and the phase transition is similar to those of Ising and Kosterlitz–Thouless systems [1–3]. In zero external field, both symmetry breakings occur at the same temperature, and the common feature transition is a multicritical point describing the confluence of two universalities.

$CsMnBr_3$ crystallizes into a hexagonal lattice, with space group $P6_3/mmc$, and with lattice parameters $a = 7.61$ Å and $c = 6.52$ Å [4], as illustrated in figure 1. The antiferromagnetic superexchange interaction ($J_0 = 0.88$ meV) between the neighbouring Mn spins along the *c*-axis is about 460 times stronger than that in the *ab*-plane ($J = 0.0019$ meV) [5–6]. For this reason, the Mn spins form infinite linear chains along the *c*-axis. At low temperatures, an in-plane anisotropy ($D = 0.014$ meV) mainly due to dipolar interaction restricts the magnetic moments in the *ab*-plane. Therefore, the system of the Mn spins in this material is approximately stacked into a triangular antiferromagnet *XY*-lattice, and the Mn spins frustrate the formation of a collinear antiferromagnetic structure. Below 8.31 K, it undergoes three-dimensional (3D) ordering. The spin configuration determined by neutron diffraction (ND) experiments is one in which the Mn spins in the *ab*-plane are rotated by 120°. However, no one has yet determined the direction of Mn spins in relation to the crystallographic axes. In order to determine the spin orientation, we have measured the Br NMR spectrum.

0953-8984/96/224063+08$19.50

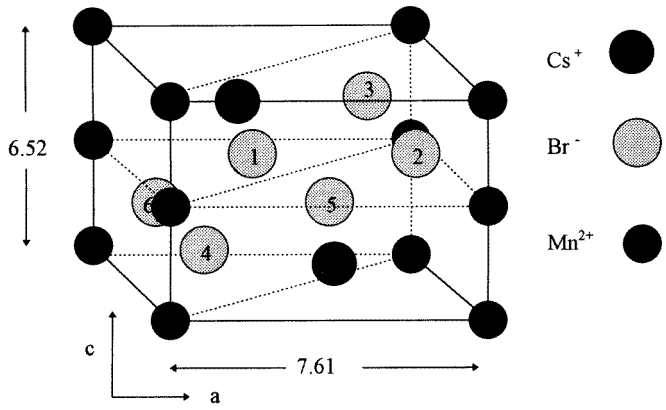

Figure 1. The unit cell of $CsMnBr_3$.

2. Experimental procedure and results

Single crystals of $CsMnBr_3$ were grown by the Bridgeman method [7]. The NMR spectra were taken with an incoherent pulsed NMR apparatus with an operating frequency ranging from 30 to 80 MHz. The NMR spectra were taken at zero field with the temperature ranging from 3.0 to 4.2 K. The resonance spectrum of the Br NMR in a single crystal of $CsMnBr_3$ was measured by the spin-echo method. In this measurement, the duration of the applied rf wave was taken to be shorter than that for the optimum intensity [8].

The Br NMR results of $CsMnBr_3$ are shown in figure 2. Figure 2(a) shows the Br NMR spectrum at 4.2 K, and figure 2(b) shows that at 3.0 K in this experiment the rf field was applied parallel to the *c*-axis. The spectrum is in the perpendicular case almost the same as that in figure 2. Distinct peaks are observed at 36.0 ± 0.5 MHz and 43.0 ± 0.5 MHz, and the measured spectrum spreads broadly from 34 to 55 MHz, although the specimen is a single crystal. Because the ratio of the two frequencies is the same as that of the quadrupole moments of ^{81}Br and ^{79}Br, we can assign the lower-frequency part of the spectrum as corresponding to the ^{81}Br resonance and the higher part as corresponding to the ^{79}Br resonance. The intensities of the two peaks are nearly equal; this reflects the natural abundance ratio of $50.57\%(^{79}\text{Br})/49.43\%(^{81}\text{Br}) \simeq 1$.

The temperature independence of the peak frequencies suggests that the observed resonance frequencies of spin-echo signals are determined mainly by the electric quadrupole interaction between the Br nucleus and surrounding ions. This broad width of the spectrum is suggested to be originating from the distribution of the internal field at the Br nuclear site.

3. Analysis and discussion

To analyse the NMR spectra, it is necessary to calculate the nuclear Hamiltonian of the Br nucleus ($I = 3/2$), which can be written as a sum of the pure quadrupole Hamiltonian and the Zeeman Hamiltonian:

$$\mathcal{H} = \frac{e^2qQ}{4I(2I-1)}[3I_z^2 - I(I+1) + \eta(I_x^2 - I_y^2)] - \gamma\hbar(\boldsymbol{B}\cdot\boldsymbol{I}) \qquad (1)$$

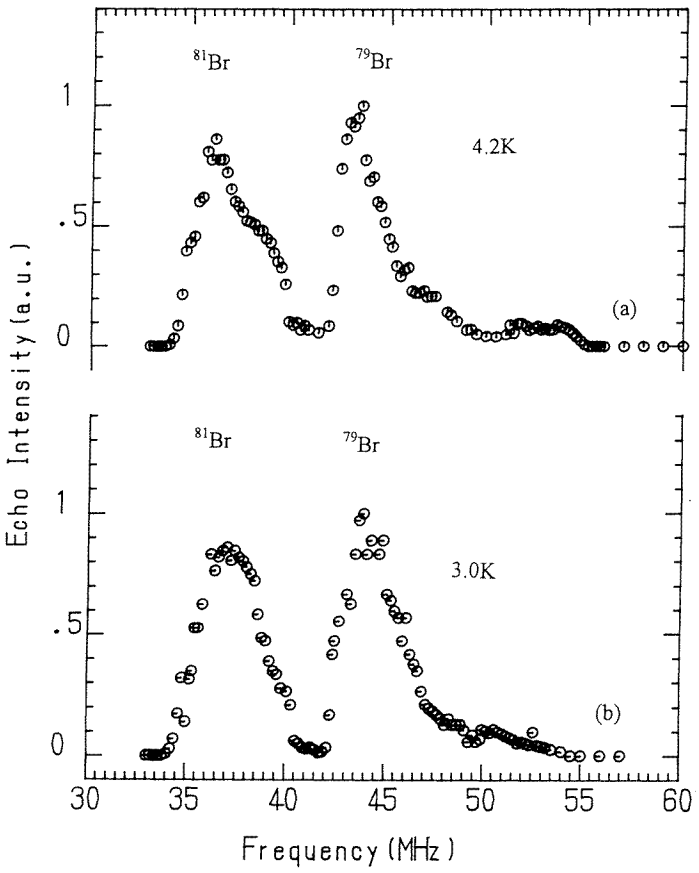

Figure 2. Spectra (a) and (b) show the Br NMR spin-echo spectra at 4.2 K and 3.0 K, respectively.

where the x-, y-, and z-axis are taken as the principal axes of electric field gradient V_{ij}, $e :=$ elementary electric charge, $q := V_{zz}/e$, $\eta := (V_{xx} - V_{yy})/V_{zz}$, $Q :=$ the electric quadrupole moment of the Br nucleus, and $\gamma :=$ the gyromagnetic constant of the Br nuclear magnetic moment. The elements of electric field gradient (EFG) were calculated under an assumption that the real charge distribution can be replaced by a set of point charges. The contribution of about 2×10^5 atoms within a sphere of radius 60 Å to the EFG is taken into account, and the calculated principal values at the Br(4) site in figures 1 and 3 are $V'_{xx}/e = 1.12 \times 10^{-25}$ (cm^{-3}), $V'_{yy}/e = 2.02 \times 10^{-26}$ (cm^{-3}) and $V'_{zz}/e = -1.32 \times 10^{-25}$ (cm^{-3}). Figure 3 represents the projection of Br and Mn atoms on the c-plane, and y and z stand for the crystallographic c-axis and a-axis, respectively. As inferred from the position of the Br nucleus, the principal value of the EFG along the c-direction is small and the asymmetry parameter η is fairly large, $|\eta| = 0.69$. It is widely known that the wave function of inner-core electrons of the Br atom is deformed by an electric field. The V_{ij}, which are determined by the experiment, can be expressed as $V_{ij} = V'_{ij}(1 - \gamma_\infty)$, where γ_∞ is called Sternheimer's antishielding factor and is isotropic [9]. Therefore, it is assumed that the asymmetry parameter η is fixed, and V_{zz} is one of the adjustable parameters to be determined by experiment.

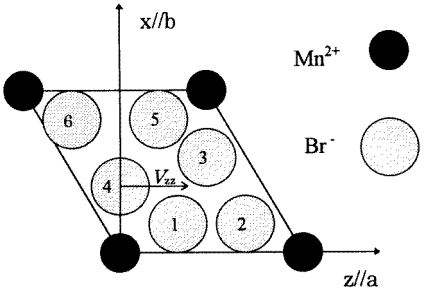

Figure 3. The projection of Br and Mn atoms onto the *ab*-plane. The Br atoms 1–6 correspond to those in figure 1. On Br(4), the principal axes of the field gradient tensor are the *x*-, *y*- and *z*-axis.

In the Zeeman interaction, the internal magnetic field at the Br site is a sum of the dipolar field and the transferred hyperfine field. In calculating the dipolar field, the magnetic moments of Mn^{2+} ions are replaced by point dipole moments. At the Br site in $CsMnBr_3$, the point dipole field was calculated as a sum of the dipole fields generated by the Mn spins (S) in a sphere of radius 60 Å with S reduced by 34% [10]. The resulting field at the Br site is about 0.08 T, which is too small to explain the experimental data.

The transferred hyperfine interaction is usually expressed as a spherically symmetrical term in the nuclear Hamiltonian. The two Mn spins nearest to the Br nucleus are coupled antiparallel to each other because of the strong antiferromagnetic interaction along the *c*-axis. In this case, the field produced by the symmetrical interaction is cancelled. The field produced by the anisotropic transferred hyperfine interaction is calculated from the following model: the Hamiltonian of the hyperfine interaction between the electronic spin $\boldsymbol{S}$ and the nuclear spin $\boldsymbol{I}$ is written as $\sum S_i A_{ij} I_j$ where A_{ij} are the coupling coefficients, which are second-rank Cartesian tensors. Tensors are reducible with respect to transformations of the coordinate system such as rotation and inversion [11]; therefore, tensors can be expressed as linear combinations of irreducible tensors as scalar, pseudo-vector and symmetric second-order (pseudo-dipolar) tensors. The transferred hyperfine interaction originates from the overlap of d-electronic wave functions of the magnetic Mn^{2+} ion with the neighbouring diamagnetic Br^- ion [12]. Therefore, the field is inversely proportional to the distance r between two atoms. When the A_{ij}-coefficients are expanded in a power series of r, the pseudo-vector term must be zero due to the antisymmetry. As a result, the coefficients T_{ij} of the anisotropic transferred hyperfine interaction are given by

$$T_{ij} = \frac{1}{2}\left[A_{ij} + A_{ji} - \frac{2}{3}A(r)\delta_{ij}\right] = f(r)\left(x_i x_j - \frac{1}{3}\delta_{ij}\right) \tag{2}$$

where $A(r) = \frac{1}{3}(A_{xx} + A_{yy} + A_{zz})$, $f(r)$ is a function of r, and δ_{ij} is the Kronecker delta. Because $f(r)$ decreases rapidly as a function of r, only the contribution of the nearest Mn^{2+} ions to the internal field is taken into consideration. Here, we use the maximum internal field B_0 instead of $f(r)$, the B_0 which is one of the adjustable parameters to be determined by experiment.

In order to examine the magnetic structure theoretically, we assumed the following two models, accomplished by computer simulation.

Firstly, we supposed a model in which the Mn spins are coupled antiferromagnetically along the *c*-axis and point in various directions in 3D; in this case, the Mn spins are in the

3D random state. The resonance frequencies and the intensities of ^{79}Br were calculated in the following way.

(i) The azimuth and the latitude of the direction of the Mn spin were determined independently by random numbers (but the word random does not fully qualify the random number: a set of random numbers between 0 and 2π is used for the azimuth angle φ, and a set of random numbers between -1 and $+1$ is used for $\cos\theta$, where θ is the latitude angle).

(ii) The internal magnetic field $\boldsymbol{B}$ at the Br site was calculated from equation (2) with these angles, where the maximum internal field B_0 is assumed to be equal to 0.3 T.

(iii) Assuming $e^2qQ/h = 88$ MHz and $|\eta| = 0.69$, we calculated the eigenvalues, the eigenfunctions of the nuclear Hamiltonian, the resonance frequency and the intensity of the ^{79}Br NMR. The many bars in figure 4(a) show the resonance of ^{79}Br, where only one hundred spins are taken into account because of the computer storage. The calculated results, unfortunately, do not reproduce the experimental data.

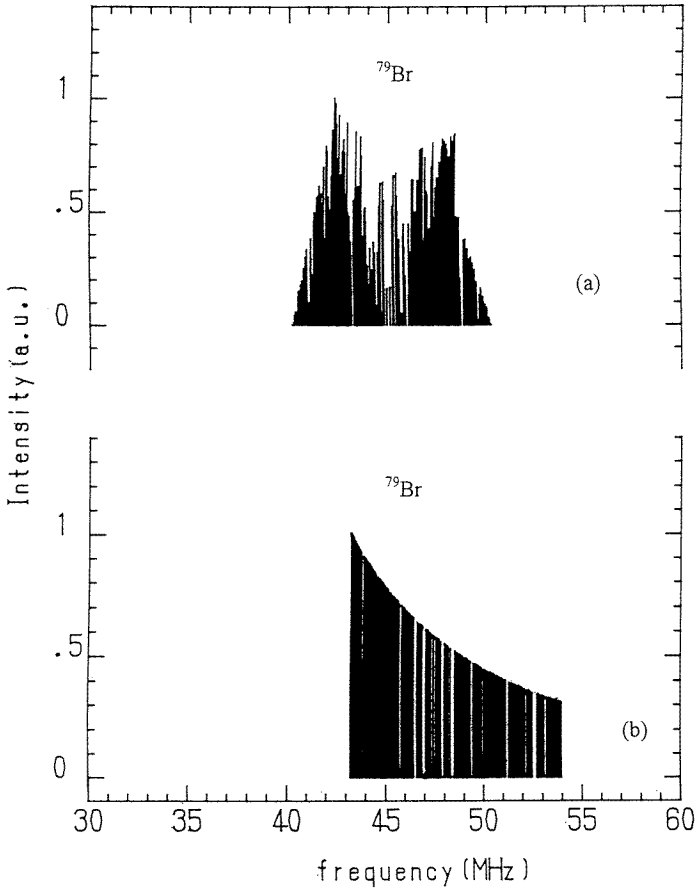

Figure 4. (a) Calculated resonance lines of ^{79}Br NMR with a model in which the spins are in a three-dimensional random state. (b) Calculated resonance lines of ^{79}Br NMR with the two-dimensional spin arrangement produced by Monte Carlo simulation.

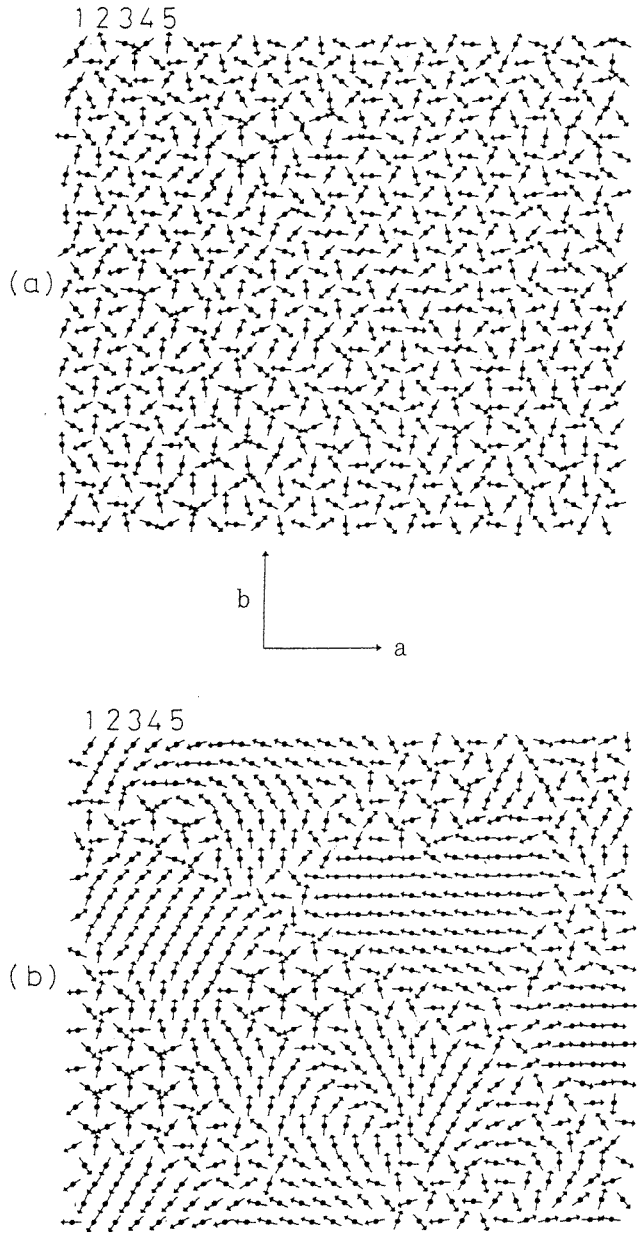

Figure 5. (a) An illustration by the Monte Carlo simulation of spins in one of the planes of the stacked triangular-lattice XY-antiferromagnet (26×26 spins $\times$ 10 planes). (b) The method for obtaining (b) from (a) is as follows: first, we number the spins in (a) from the left to the right (in (a) the first five spins are numbered); then, we rotate the Nth spin by $(N-1) \times 120^\circ$. That is, the direction of spin No 1 is not changed. That of spin No 2 is increased by 120°. Spin No 3 is rotated by 240°, or -120°, and so on. After rotating the spins in this manner, we have (b).

As the second model we take one where the Mn spins are coupled antiferromagnetically along the c-axis and point to various directions in the c-plane. We have performed a

Monte Carlo simulation using a configuration of the actual crystal. The model is a stacked triangular-lattice antiferromagnet with a finite size (26×26 spins and 10 planes). The calculation is based on the Metropolis method applied to the spin system of the model, where the exchange parameters equal those of $CsMnBr_3$ but the Mn spins lie in the c-plane. We have assumed that the temperature can be expressed as $0.001 \times 2J_0S^2/\kappa_B$ where κ_B is the Boltzmann constant, and the number of iterations is about 70 millions/spin. The calculated results are shown in figure 5(a).

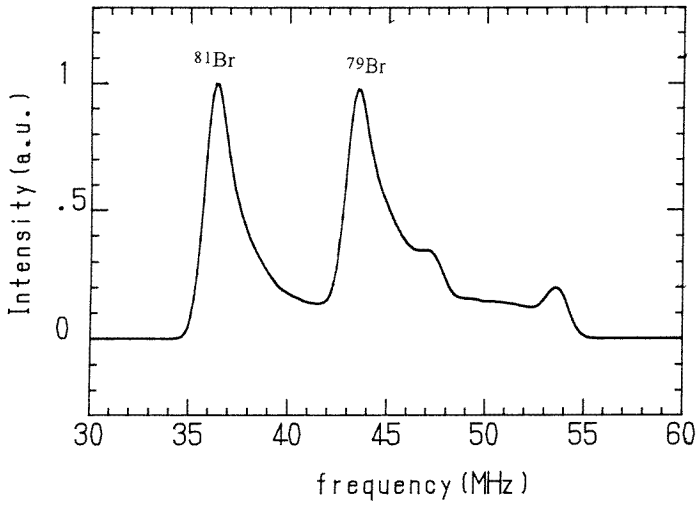

Figure 6. The theoretically calculated spectrum of Br NMR in zero external field.

The method for obtaining figure 5(b) from figure 5(a) is as follows. First, we number the spins in figure 5(a) from the left to the right and from the top to the bottom. (In figure 5(a) the first five spins are numbered.) Then, we rotate the Nth spin by $(N-1) \times 120^\circ$. After rotating the spins in this manner, we have figure 5(b). The configuration of spins in figure 5(b) is just the same as that in figure 5(a). Entire areas of figure 5(b) can be separated into region A containing trains of spins and region B including Y-like combinations of spins. Although the spins in regions A and B are oriented in different fashions, we can see that the total system in the c-plane is in the disordered state.

Taking the second model, we calculated the ^{79}Br NMR spectrum via the following scheme.

(i) The internal field at the Br site is calculated with the angle between the spin and the b-axis in figure 5(a), and with $B_0 = 0.51$ T, which is estimated from the separation between the maximum and the minimum frequencies of the experimental data. Here, the internal field is parallel to the c-axis from equation (2).

(ii) Assuming $|\eta| = 0.69$, the principal value of the EFG is determined by the lowest frequency of the spectrum, that is, $e^2qQ/h = 88$ MHz.

(iii) Using these parameters, we calculated the resonance frequency and the intensity of the ^{79}Br NMR. The calculated results are shown in figure 4(b), where bars show the resonance; and the bars are dense in the vicinity of the lowest frequency.

The intensity of the spectrum depends on the bar density; however, we could not understand the convolution directly from figure 4(b). It is noted that, in our experiment,

the NMR spectra are taken by an incoherent pulsed NMR method. This means that we can employ a set of Gaussian functions, whose common width is $1/\Delta t$ (Δt is the duration of application of the rf wave, approximately equal to 1.0 μs). Figure 6 illustrates the simulation results, and our NMR data support such a complicated structure. The ND experimental data are also consistent with this figure because it reflects the regular structure in the range of the coherence length of the ND.

4. Conclusions

In conclusion, the broad width of the Br NMR spectrum is considered to be arising from the distribution of the internal field at the Br site due to the frustration effects. We have shown that $CsMnBr_3$ has a disordered magnetic structure in two dimensions, namely, that the spins are coupled antiferromagnetically along the *c*-axis and are pointing in various directions in the *c*-plane. This disordered state may vanish close to the ground state. In order to investigate the ground state further, we need to perform NMR experiments at lower temperature.

Acknowledgments

We would like to thank Professor M Chiba (Kyoto University), Professor F Kai (Kumamoto University) and Dr Alex Lacerda (National High Magnetic Field Laboratory, Los Alamos Facility) for their critical reading of the manuscript and discussions. We also thank Mr T Shimamoto for help with the numerical computation.

References

[1] Miyashita S and Shiba H 1984 *J. Phys. Soc. Japan* **53** 1145
[2] Kawamura H 1986 *J. Phys. Soc. Japan* **55** 2095
[3] Lee D H, Joannopoulous J D and Negele J W 1986 *Phys. Rev.* B **33** 450
[4] Goodyear J and Kennedy D J 1974 *Acta Crystallogr.* B **28** 1640
[5] Gaulin B D, Collins M F and Buyers W J L 1987 *J. Appl. Phys.* **61** 3409
[6] Gaulin B D, Mason T E, Collins M F and Larese J Z 1989 *Phys. Rev. Lett.* **62** 1380
[7] Zaliznyak I A, Prozorova L A and Petrov S V 1990 *Sov. Phys.–JETP* **70** 203
[8] Slichter C P 1990 *Principles of Magnetic Resonance* (Berlin: Springer) pp 35–50
[9] Lucken E A C 1969 *Nuclear Quadrupole Coupling Constants* (New York: Academic) pp 88–95
[10] Falk U, Furrer A, Gudel H U and Kjems J K 1987 *Phys. Rev.* B **35** 4888
[11] Rose M E 1957 *Elementary Theory of Angular Momentum* (New York: Wiley) p 76
[12] Shrivastava K N 1975 *Phys. Rep.* **20** 137